Lewis acid effects on donor–acceptor associations and redox reactions: ternary complexes of heteroaromatic *N*-oxides with boron trifluoride and organic donors†

Yakov P. Nizhnik,‡ Jianjiang Lu, Sergiy V. Rosokha*§ and Jay K. Kochi¶

Received (in Montpellier, France) 20th May 2009, Accepted 28th July 2009
First published as an Advance Article on the web 22nd September 2009
DOI: 10.1039/b9nj00205g

Structural and spectral features of the novel supramolecular [D·NXO·BF_3] complexes formed *via* simultaneous n-coordination of a Lewis acid (BF_3) and π-complexation of organic donors (D) to polyfunctional nitrosubstituted *N*-oxide molecules (NXO = 4-nitropyridine-*N*-oxide or 4-nitroquinoline-*N*-oxide) are reported. X-Ray studies of [pyrene·NPO·BF_3]·CH_2Cl_2 and [$(pyrene)_2$·NQO·BF_3] salts revealed that the Lewis acid is coordinated to the oxygen atom of the *N*-oxide group with O–B distance of ~1.52 Å similar to that in the separate [NXO·BF_3] adducts. Aromatic rings of *N*-oxide molecules in the ternary systems are π-stacked with pyrene moieties, and their interplanar separations of ~3.35 Å are common for conventional charge-transfer complexes. In dichloromethane, associations between [NXO·BF_3] adduct and organic donors are characterized by higher formation constants (and charge-transfer bands of [D·NXO·BF_3] complexes are red-shifted) as compared to the complexes between the same donors and NXO acceptors. Spectral data and electrochemical measurements point out enhanced acceptor abilities of [NXO·BF_3] adducts relative to the separate *N*-oxides which correspond to ~0.5 V positive shift of reduction potentials of acceptors. Synergetic oxidation of strong organic donors by [NXO·BF_3] dyads (which results in the formation of the corresponding cation radicals and products of transformation of both BF_3 and NXO components) is discussed.

1. Introduction

Lewis acid catalysis is a common method of activation of various organic reactions, in particular chemical transformations involving an electron-transfer step.[1–3] Catalysis of the latter usually occurs *via* (a) an electron abstraction from a donor by a Lewis acid, (b) assembly of Lewis acids and bases together with metal ions that undergo redox process, and (c) formation of Lewis acid adducts with oxidizing or reducing agents (which enhances their reactivity).[3] Besides, Fukuzumi and co-workers reported recently that addition of a Lewis acid (metal ions) accelerates drastically electron-transfer-activated reactions.[4] This was assigned primarily to the coordination of the Lewis acid with the anionic products of the redox process which resulted in the positive shift of redox potential of acceptors, and thus, in favorable modulation of the overall thermodynamics of the electron-transfer step.[4]

In order to clarify the mechanistic role of a Lewis acid in a redox process, it is essential to determine its binding site and its effects on reactants, intermediates and/or products. Of particular interest in this respect is a Lewis acid binding with the key intermediate of intermolecular electron-transfer processes, a precursor complex.[5] We have shown recently that analysis of the spectral and structural features of the (donor–acceptor) precursor complexes provides important insight into the potential energy surfaces (and thus mechanism) for the various organic self- and cross-exchange redox reactions.[6] Thus, experimental evaluation of the corresponding characteristics of associates involving a donor, an acceptor and a Lewis acid is expected to provide valuable information for the elucidation of the catalytic redox processes. However, quantitative spectral and structural data on these ternary complexes are lacking (in spite of the fact that some indications of the Lewis acid enhancement of the acceptor abilities of nitrobenzenes in their association with organic donors were reported more than 50 years ago).[7] In search for the donor–acceptor–Lewis acid components for ternary supramolecular associates, we turn to the nitrosubstituted *N*-oxides (designated hereinafter as NXO, where X = Q for 4-nitroquinoline-*N*-oxide and X = P for 4-nitropyridine-*N*-oxide, see Chart 1).

This choice is determined by the dual nature of nitrosubstituted *N*-oxides in Chart 1, which contain both aromatic parts with mild π-acceptor properties appropriate for the charge-transfer complexation with organic donors and

Department of Chemistry, University of Houston, Houston, TX 77204, USA

† Electronic supporting information (ESI) available: IR, UV-Vis spectral data and cyclic voltammograms of NXOs, BF_3 and their mixtures, pyrene–NXO stacking in X-ray structures, resonance contributors to *N*-oxide structure. CCDC 742367, 742368 and 743147–743149. For ESI and crystallographic data in CIF or other electronic format see DOI: 10.1039/b9nj00205g

‡ Current address: Department of Molecular Biology, Biological and Organic Chemistry, Petrozavodsk State University, Pr. Lenina 33, Petrozavodsk, 185910, Russia. E-mail: yakov_nizhnik@mail.ru
§ Current address: Department of Biological, Chemical and Physical Sciences, Roosevelt University, 430 S. Michigan Ave, Chicago, IL 60605, USA. Tel: +1 847-670-1595, Fax: +1 847-619-8555. E-mail: srosokha@roosevelt.edu.
¶ Deceased, August 9, 2008.

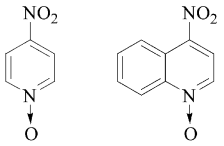

NXO: NPO NQO

Chart 1

N-oxide groups suitable for Lewis acid coordination. Indeed, NQO acceptor forms charge-transfer complexes with DNA, proteins and their components, and other donors,[8] and this complexation was considered as a major factor in the biological activity of 4-nitroquinoline-*N*-oxide.[9] [Note that NQO represents a model carcinogen for studies of the mechanism of carcinogenicity and mutagenicity,[10] apoptosis,[11] as well for the evaluation of the anticarcinogenic properties of various substances, *e.g.* polyphenols from green tea and fermented milk.][12] Furthermore, it was shown that S_NAr reactions of *N*-oxides (which are important precursors in the heterocyclic chemistry[13]) are drastically accelerated in the presence of Lewis acids.[14] UV-Vis/IR spectral data revealed the formation of complexes between various *N*-oxides and boron trifluoride, but their structural features remained ambiguous.[15]

In the current work, we report structural and spectral features of the novel ternary complexes[16] formed *via* simultaneous n-coordination of boron trifluoride (Lewis acid) and π-complexation of organic donors to polyfunctional NQO and NPO molecules, and discuss how coordination of a Lewis acid affects optical and thermal electron-transfer processes in these donor–acceptor systems.

2. Experimental

2.1 Materials

Commercially available tetracyanoquinodimethane, tetrafluorotetracyanoquinodimethane, *p*- and *o*-chloranils, *p*- and *o*-bromanils, *p*-fluoranil, tetracyanoethylene, *p*-benzoquinone, 2,3-dicyano-*p*-benzoquinone, 2,6-dichloro-*p*-benzoquinone, 2,3-dichloro-5,6-dicyano-*p*-benzoquinone, 2,3-dibromo-5,6-dicyano-*p*-benzoquinone acceptors, as well as hexamethylbenzene, hexaethylbenzene, pentamethylbenzene, naphthalene, *p*-dimethoxybenzene, anthracene, pyrene, 9,10-dimethylanthracene, octamethylbiphenylene and tetrathiafulvalene (TTF) donors were used without additional purification. Tetracyanopyrazine was a gift from Dr J. F. Neumer (DuPont Co). Phenothiazine (PTZ) was recrystallized from toluene, and tetramethyl-*p*-phenylenediamine (TMPD) was sublimed *in vacuo*. Solutions of BF_3 in acetonitrile were prepared by passing gaseous BF_3 through dry acetonitrile. Concentrations of BF_3 in acetonitrile and in the commercially available $BF_3{\cdot}Et_2O$ solutions were determined by their titration as described earlier.[17] 4-Nitroquinoline-*N*-oxide (NQO) and 4-nitropyridine-*N*-oxide (NPO) were synthesized from quinoline and pyridine *N*-oxides as described earlier.[13,18] Dichloromethane and acetonitrile were purified according to the published procedures.[19]

2.2 Measurements and computations

UV-Vis measurements were carried out with a HP-845 UV-Vis spectrophotometer. Formation constants and extinction coefficients were evaluated *via* the Benesi–Hildebrand and Drago procedures,[20] and/or by minimizing differences between experimental and calculated absorbances of solutions at different concentrations of reactants as described earlier.[21] Cyclic voltammetry (CV) was performed with a BAS 100A electrochemical analyzer equipped with a platinum electrode under an argon atmosphere with Bu_4BF_4 supporting electrolyte.[21] IR spectra of neat crystalline materials were recorded on a Nicolet 10 DX FT spectrometer using single-reflection HATR (Smart Miracle). GC-MS studies were carried out with an Agilent 6890 GC system with a 5973 mass selective detector. Frontier orbitals were evaluated *via* single-point B3LYP/6-311* Gaussian 98[22] computation using Cube = (55, orbital) option and atomic coordinate from the corresponding X-ray structure.

2.3 Crystallization—$(pyrene)_2{\cdot}NPO$

70 mg of 4-nitropyridine-*N*-oxide (0.50 mmol) and 202 mg of pyrene (1.0 mmol) were dissolved in 2 mL of dichloromethane. The resulting solution was cooled to −78 °C, which led to formation of yellow plates suspended at the surface of the liquid and a small amount of microcrystalline material on the bottom of the vial. After separation of the microcrystals by centrifugation, the remaining solution containing floating plates was filtered, and the yellow crystals were dried in air. Single-crystal X-ray study revealed 2 : 1 pyrene–NPO stoichiometry of this salt (see crystallographic parameters and details of structure refinements in Table 1). IR data for this salt (together with those for separate NQO and pyrene) are listed in Table S1 in the ESI.†

2.4 $NPO{\cdot}BF_3$

200 μL (1.6 mmol) of $Et_2O{\cdot}BF_3$ were added to the solution of 140 mg (1.0 mmol) of 4-nitropyridine-*N*-oxide in dichloromethane. It resulted in the precipitation of a colorless crystalline material, which was filtered, washed with 1 mL of dichloromethane and dried in a desiccator over P_2O_5 powder and paraffin oil (see crystallographic and IR data in Table 1 and Table S1 in ESI,† respectively).

2.5 $NQO{\cdot}BF_3$

63 μL (0.50 mmol) of $Et_2O{\cdot}BF_3$ were added to the solution of 95 mg (0.50 mmol) of 4-nitroquinoline-*N*-oxide in 3 ml of CH_2Cl_2. Evaporation of the major portion of the solvent in a desiccator (over paraffin oil and P_2O_5) led to formation of large yellow needles. The rest of the solvent (~0.5 mL) was decanted, and crystals were washed with diethyl ether (Table 1 and Table S2 in ESI†).

2.6 $Pyrene{\cdot}NPO{\cdot}BF_3{\cdot}CH_2Cl_2$

30 μL (0.24 mmol) of $Et_2O{\cdot}BF_3$ were added to the solution of 28 mg (2.0 mmol) of NPO and 81 mg (4.0 mmol) of pyrene in 3 mL of dichloromethane. It resulted in a red-brown coloration of the solution. In few minutes, colorless crystals of $NQO{\cdot}BF_3$ complex were formed and the coloration almost disappeared. This heterogeneous system was kept at −30 °C, and large

Table 1 Crystallographic parameters and the details of the structure refinements

Compound	$(Pyrene)_2$·NPO	NPO·BF_3	Pyrene·NPO·BF_3·CH_2Cl_2	NQO·BF_3	$(Pyrene)_2$·NQO·BF_3
Formula	$C_{37}H_{24}N_2O_3$	$C_5H_4BF_3N_2O_3$	$C_{22}H_{16}BCl_2F_3N_2O_3$	$C_9H_6BF_3N_2O_3$	$C_{82}H_{52}B_2F_6N_4O_6$
FW	544.58	207.91	495.08	257.97	662.45
Crystal system	Triclinic	Orthorhombic	Monoclinic	Orthorhombic	Monoclinic
Space group	$P\bar{1}$	$Pca2_1$	$P2_1/c$	$P2_12_12_1$	$P2_1$
a/Å	8.1578(16)	11.996(3)	7.0332(14)	5.4823(9)	14.799(3)
b/Å	8.2030(16)	6.0475(13)	10.3535(19)	12.217(2)	8.1970(14)
c/Å	10.141(2)	11.156(2)	29.588(6)	15.168(3)	25.036(5)
α/°	89.462(4)	90.00	90.00	90.00	90.00
β/°	76.889(4)	90.00	91.623(5)	90.00	90.744(5)
γ/°	80.215(4)	90.00	90.00	90.00	90.00
V/Å^3	651.0(2)	809.3(3)	2153.7(7)	1015.9(3)	3036.8(10)
Z	1	4	4	4	4
d_{calcd}/g cm^{-3}	1.389	1.706	1.527	1.687	1.449
μ/mm^{-1}	0.089	0.177	0.356	0.159	0.103
n measd	9011	7360	24 464	6559	31 925
n ind	3789	2319	6358	2956	14 640
n obs ($I \geq 2\sigma(I)$)	2386	1643	3107	2073	7477
R ($I \geq 2\sigma(I)$)	0.0572	0.0493	0.0784	0.0504	0.0802
R_w ($I \geq 2\sigma(I)$)	0.1502	0.0919	0.1912	0.0954	0.1716
GOF	1.022	1.004	1.028	1.012	1.057

dark-red crystals were formed after 1 week (Table 1 and Table S1, ESI†). Exposure of the dark-red crystals to air resulted in their decomposition (in 10–15 min) and formation of a white residue.

2.7 $(Pyrene)_2$·NQO·BF_3

30 μL (0.24 mmol) of Et_2O·BF_3 were added to the solution of 36 mg (2.0 mmol) of NQO and 81 mg (4.0 mmol) of pyrene in 3 mL of acetonitrile. The resulting red-brown solution was cooled to −30 °C. This led to formation of reddish-black crystals together with a small amount of microcrystalline yellow sediment. After one week, the latter disappeared and only large reddish-black crystals remained in the solution (Table 1 and Table S2 in ESI†).

2.8 X-Ray Crystallography

Intensity data for X-ray crystallographic analysis were collected at 173 K with a Bruker SMART Apex diffractometer using MoKα radiation (λ = 0.71073 Å). The structures were solved by direct methods and refined by full matrix least-squares treatment.[23] Crystallographic details for the binary and ternary salts of NQO or NPO *N*-oxides with BF_3 and/or pyrene donor are listed in Table 1.

3. Results and discussion

3.1 Structural characterization of binary and ternary complexes

3.1.A Binary [NXO, BF_3] complexes. X-Ray crystallography of binary [NPO·BF_3] and [NQO·BF_3] complexes showed coordination of BF_3 to the *N*-oxide group (Fig. 1) with B–O distances of ~1.52 Å (Table 2), which are in the same range as those in the boron trifluoride adducts with various n-donors.[24] The dihedral C5–N1–O1–B1 angle of 78.4(3)° in [NPO·BF_3] and the C5–N1–O1–B1 angle of 81.6(3)° in [NQO·BF_3] point out the sp^3 hybridization of oxygen atoms of the *N*-oxide in these complexes.[25]

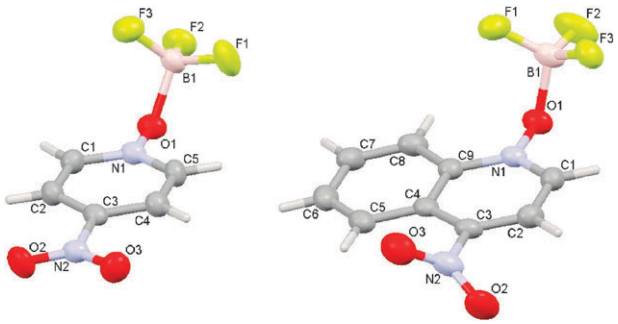

Fig. 1 Molecular structure of the [NPO·BF_3] (left) and [NQO·BF_3] (right) adducts (Note: ellipsoids are drawn at 50% probability level).

Analysis of the molecular structures of *N*-oxides in the [NPO·BF_3] and [NQO·BF_3] adducts (Table 2) indicates that Lewis acid binding leads to significant elongation (~0.075 Å) of the N1–O1 bonds, as compared to the corresponding values in the isolated NXO molecules. Besides, BF_3-coordinated moieties are characterized by less bond length variation within pyridine rings, by longer C3–NO_2 bonds and by larger nitro group twist angles (Table 2). Such structural changes indicate that Lewis acid coordination results in some decrease of the quinonoidal character of *N*-oxide molecules.[26]

3.1.B Donor–acceptor complexes of NPO with pyrene. Cooling or evaporation of solutions containing NXO acceptors and organic donors (various alkybenzenes, naphthalenes, anthracenes, *etc.*) led to crystallization of separate starting materials, except for the solutions containing NPO and pyrene. The latter afforded yellow crystals, and their X-ray measurements showed stacks of interchanging pyrene and NPO molecules. These stacks are separated by additional arenes, so the overall NPO to donor ratio is 1 : 2 (Fig. 2). All three components lie on inversion centers in this structure (which results in disorder for the NPO molecule).

In this structure, NPO moieties are located in the "cavities" formed by four pyrene molecules (two of which are almost parallel, and two are nearly perpendicular to NPO plane).

Table 2 Selected bond distances (Å) and angles (°) for NPO and NQO molecules[a]

Bond lengths and angles	NPO[b]	NPO·BF_3	$(Pyrene)_2$·NPO[c]	$(Pyrene)_2$ ·NPO·BF_3	NQO[d]	NQO·BF_3	Pyrene·NQO·BF_3[e]
N1–O1	1.291(2)	1.368(3)	1.343(18)	1.375(3)	1.293(4)	1.370(3)	1.352(5)/1.358(5)
N1–C1	1.370(2)	1.350(4)	1.306(14)	1.338(4)	1.342(4)	1.320(3)	1.331(6)/1.307(6)
N1–C5[f]	1.369(2)	1.340(4)	1.376(10)	1.342(4)	1.420(4)[e]	1.384(3)[e]	1.386(5)/1.385(6)[e]
C3–NO_2	1.458(2)	1.478(3)	1.51(2)	1.484(4)	1.464(4)	1.480(3)	1.470(6)/1.492(6)
N2–O2	1.230(2)	1.218(4)	1.162(17)	1.209(4)	1.236(4)	1.220(3)	1.219(5)/1.181(6)
N2–O3	1.223(2)	1.222(4)	1.252(14)	1.227(4)	1.222(4)	1.231(3)	1.216(5)/1.179(6)
C1–C2	1.377(3)	1.371(4)	1.380(10)	1.376(4)	1.385(5)	1.393(3)	1.376(7)/1.391(7)
C2–C3	1.387(3)	1.376(4)	1.331(12)	1.371(4)	1.360(5)	1.354(3)	1.361(6)/1.358(7)
C3–C4	1.388(2)	1.378(4)	1.397(8)	1.376(4)	1.427(4)	1.415(3)	1.427(6)/1.404(7)
C4–C5[g]	1.377(3)	1.377(4)	1.391(10)	1.364(4)	1.420(4)[f]	1.420(3)[f]	1.407(6)/1.417(7)[f]
O1–B1	—	1.524(5)	—	1.518(4)	—	1.513(3)	1.511(6)/1.517(7)
∠ NO_2–Pyr[h]	0	3.39	2.81	2.12	16.73	38.47	39.53/11.67
∠ NOB–Pyr[i]	—	75.70	—	79.35	—	79.47	72.66/39.38

[a] See Fig. 1 for atom labeling. [b] Ref. 27. [c] Disordered NPO molecule. [d] Ref. 28. [e] Two crystallographically independent molecules. [f] Or N1–C9 (for NQO). [g] Or C4–C9 (for NQO). [h] Dihedral angle between O2–N2–O3 and pyridine planes. [i] Dihedral angle between N1–O1–B and pyridine planes.

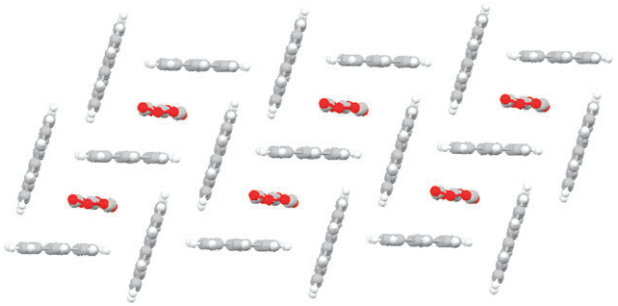

Fig. 2 Fragment of crystal structure of the $(pyrene)_2$·NPO.

Interplanar separations between nearly parallel NPO and pyrene moieties (~3.32 Å) are usual for charge-transfer salts,[29] but lateral donor–acceptor shift significantly decreases their overlap (Fig. S1 in ESI†). The distances between carbon atoms of NPO and perpendicular pyrene planes (~3.52 Å), and between pyrene hydrogens and neighboring pyrene planes (~2.722 and ~2.636 Å) point to some C–H–π (T-shaped) interactions in these crystals.

3.1.C Structural characterization of ternary complexes of *N*-oxides with BF_3 and pyrene. Cooling of the solutions containing mixtures of pyrene, *N*-oxide and Lewis acid resulted in isolation of the supramolecular associates containing all three components (see Experimental section for details). In particular, dark-red crystals of pyrene·NPO·BF_3·CH_2Cl_2 solvate showed vertical stacks in which BF_3-coordinated *N*-oxides interchange with pyrenes (Fig. 3), and NPO moieties are located over the center of neighboring donors (see Fig. S1 in ESI†). The closest donor–acceptor C···C contacts within these stacks are 3.351(4) and 3.380(4) Å (*i.e.* slightly less than their van der Waals separation of 3.40 Å).

In general, structural characteristics of NPO moieties and their bonding with BF_3 are similar to those in the NPO·BF_3 adduct (Table 2). It is noticeable that π-interaction of NPO with pyrene leads to further elongation of the N1–O1 and C3–NO_2 bond lengths, and thus to a decrease of the quinonoidal character of the *N*-oxide as compared to the analogous isolated NPO molecule.

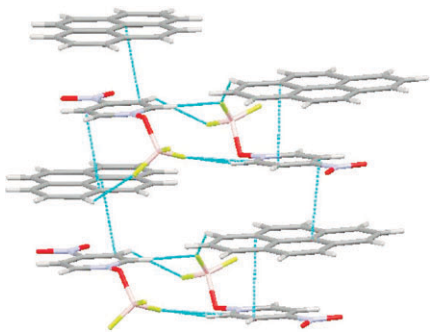

Fig. 3 Fragment of crystal structure of pyrene·NPO·BF_3·CH_2Cl_2 salt with light blue line indicating contacts shorter than the sum of the van der Waals radii (solvent molecules are omitted for clarity).

X-Ray measurement of the dark-red crystals formed in the solutions containing NQO, BF_3, and pyrene also revealed infinite stacks of [NQO·BF_3] adducts interchanging with pyrene moieties. [Note that there are two crystallographically independent pyrenes and two independent NQO moieties within these stacks, see Table 2.] These stacks form layers, which are separated by additional aromatic molecules (Fig. 4). As such, these crystals are characterized by 2 : 1 : 1 pyrene : NQO : BF_3 ratio, and T-shaped C–H–π-interactions between stacked and inter-stack pyrenes are somewhat analogous to that in $(pyrene)_2$·NPO salt.

Pyrene and *N*-oxide molecules in the stacks form two distinct donor–acceptor dyads. One of them shows two short intermolecular carbon–carbon contacts (light blue lines in Fig. 4) of 3.260(7) and 3.360(7) Å, and the other shows separations of 3.363(6) and 3.379(6) Å.

Thus, X-ray crystallographic studies of the supramolecular pyrene·NXO·BF_3 assemblies show that organic donors are π-bonded to the aromatic fragments of *N*-oxide moieties. This is consistent with the fact that the NPO·BF_3 adduct LUMO (which is critical for interaction with the donor) is located predominantly on the NPO moiety, and its shape is very similar to the LUMO shape of isolated NPO *N*-oxide (Fig. 5). [Note, however, that disordered NPO molecules in $(pyrene)_2$·BF_3 salt in Fig. 2 are stacked over the periphery of the pyrene donor, while BF_3-coordinated NPO and NQO

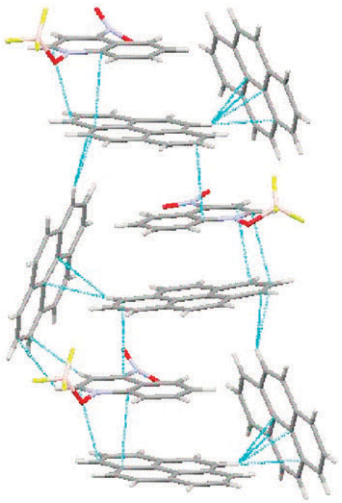

Fig. 4 Fragment of crystal structure of the (pyrene)$_2$·NQO·BF_3 with light blue line indicating contact shorter than the sum of the van der Waals radii.

molecules in Fig. 3 and 4 are stacked essentially over the center of the donor, see Fig. S1 in ESI†.] As such, these ternary associates can be considered as donor–acceptor complexes in which the properties of the *N*-oxide acceptors are modulated by the coordinated Lewis acid. To evaluate how such coordination affects the thermodynamics of donor–acceptor interactions and thermal/optical electron-transfer processes, we turn to electronic spectroscopic study in solutions, as follows.

3.2 Electronic spectroscopy of binary and ternary complexes of 4-nitrosubstituted *N*-oxides

3.2.A Binary donor–acceptor complexes. Pale-yellow solutions of NPO and NQO *N*-oxides in dichloromethane show intense absorption bands at λ = 344 and 386 nm, respectively (Table S3 in ESI†). Addition of the strong donor tetramethyl-*p*-phenylenediamine (TMPD) to either of these solutions resulted in the appearance of new absorption bands around 500 nm. In particular, addition of TMPD to solution of NPO led to the appearance of a band at 517 nm (Fig. 6A). Quantitative analysis[20,21] of the absorption intensity at various concentrations of components indicated that this band is related to formation of a 1 : 1 [TMPD, NPO] complex (eqn (1))

$$\mathrm{TMPD} + \mathrm{NPO} \overset{K_{DA}}{\rightleftarrows} [\mathrm{TMPD, NPO}] \qquad (1)$$

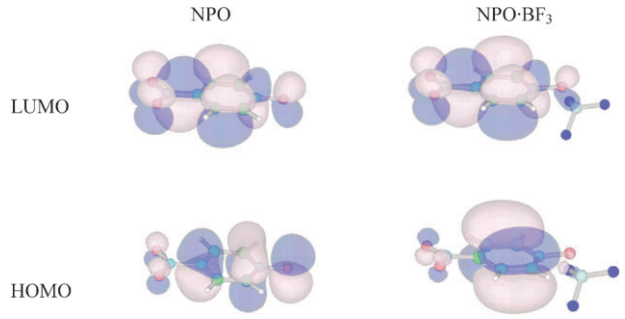

Fig. 5 Frontier orbital shape for NPO *N*-oxide and its complex with BF_3.

and afforded formation constant of K_{DA} = 1.2 M^{-1}. Similar bands in the visible range were observed when other strong donors (phenothiazine or tetrathiafulvalene) were added to the solution of either NQO or NPO acceptors. In comparison, addition of a weaker anthracene donor to the solution of NPO resulted in appearance of a broad shoulder on the low-energy tail of the strong band of the acceptor (Fig. 6B). Intensity of this absorption (measured at 450 nm) was consistent with the formation of a 1 : 1 [pyrene, NPO] complex, and its deconvolution into Gaussian components (see Fig. S2 in ESI†) produced an approximate position of the new band maximum at $\lambda_{max} \approx$ 425 nm. An analogous broad shoulder on the low-energy tail of NPO was observed with pyrene (Fig. S3 in ESI†). Formation constants for the complexes of NPO with strong organic donors are listed in Table 3. [Note that an intense absorption band of NQO at λ = 386 nm hindered quantitative analysis of complexation of this acceptor with most of the donors.]

UV-Vis measurements of the solutions containing NXO *N*-oxides and one of the weaker donors (*e.g.* alkylbenzenes or naphthalenes) did not reveal any new absorption bands. This observation accords with Mulliken's theory[29] which predicts that absorption bands (if any) for complexes with weaker donors are expected at higher energies, where they are apparently overshadowed by absorption of NXO acceptors and/or organic donors.

3.2.B Binary acceptor–Lewis acid complexes. Earlier studies established that interaction of *N*-oxides with boron trifluoride results in formation of the 1 : 1 complex according to eqn (2).[15]

$$\mathrm{NXO} + \mathrm{BF_3} \overset{K_{LA}}{\rightleftarrows} [\mathrm{NXO \cdot BF_3}] \qquad (2)$$

In agreement with the reported data, our spectral measurements showed that addition of BF_3 to solutions of NPO or NQO in acetonitrile results in disappearance of the lowest-energy bands of *N*-oxides and rise of new (blue-shifted) bands of [NXO·BF_3] complex (Fig. 7, and Table S3 and Fig. S4 in ESI†).

Quantitative analysis of the spectral changes confirmed the stoichiometry in eqn (2) and afforded high values of complex formation constants of K_{LA} = 2.8 × 10^3 M^{-1} and 1.7 × 10^3 M^{-1} with NPO and NQO, respectively. Similar studies in dichloromethane showed that equilibria in eqn (2) are shifted to the right with $K_{LA} > 10^4$ M^{-1}, and essentially complete coordination of *N*-oxide molecules with BF_3 occurs if significant excess of Lewis acid is added to 1–10 mM solutions of NXOs.

3.2.C Ternary donor– acceptor–Lewis acid complexes. Addition of anthracene donor to the dichloromethane solution containing NPO *N*-oxide and excess of boron trifluoride led to appearance of a new band with a distinct maximum at λ_{max} = 511 nm (Fig. 8). This band is red-shifted relative to the absorption of the [anthracene, NPO] complex in Fig. 6B. In view of essentially complete binding of NPO molecules with BF_3 in the solutions containing excess of Lewis acid (and since further addition of boron trifluoride did not affect spectra), we

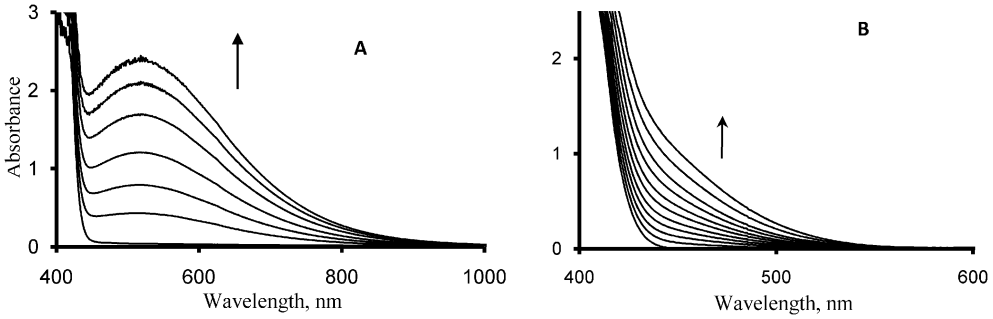

Fig. 6 Spectral changes accompanying addition of TMPD (A) and anthracene (B) donors to the dichloromethane solutions of NPO acceptor. Concentrations of components: (A) 0.2 M NPO and from 0.0 to 1.2 M TMPD. (B) 0.12 M NPO and from 0.0 to 0.14 M anthracene.

Table 3 Spectral characteristics and formation constants for complexes between various donors and NPO or NPO·BF_3 acceptors (CH_2Cl_2, 22 °C)

		Acceptor			
		NPO		NPO·BF_3	
Donor	$E_{ox}^{1/2}$ [a]/V	K_{DA}/M^{-1}	λ_{max} (ε)	K_{DAL}/M^{-1}	λ_{max} (ε)
TMPD	+0.12	1.2	518 (110)	[b]	[b]
PTZ	+0.59	1.0	480 (55)	[b]	[b]
Anthracene	+1.09	0.3[c]	425[cd]	1.0	511 (430)
Pyrene[f]	+1.16	0.3[c]	—	0.7	500 (550)

[a] From ref. 6. [b] Cation radical absorption was observed (see text). [c] Band maximum was overshadowed by NPO absorption, and K was estimated from absorption changes at λ = 450 nm. [d] λ_{max} was estimated from spectral deconvolution. [e] In comparison, K_{DA} = 0.5 M^{-1} for complex of pyrene with NQO. [f] In comparison, λ_{max} = 510 nm and K_{DAL} = 1.1 M^{-1} for complex of pyrene with [NQO·BF_3].

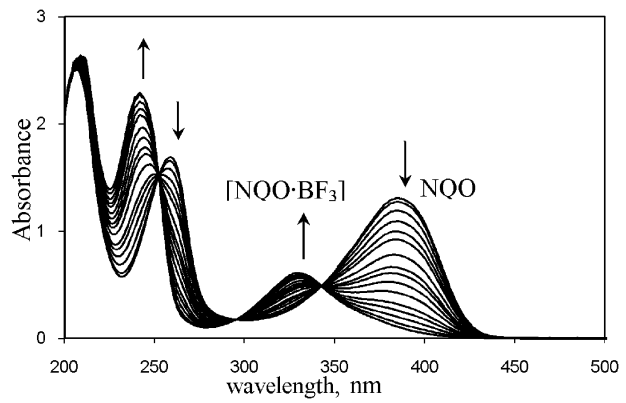

Fig. 7 Spectral changes accompanying addition of BF_3 (from 0 to the 0.5 mM solution of NQO in acetonitrile).

assigned the new band at λ = 511 nm to a complex between donor and [NPO·BF_3] adduct:

$$\text{anthracene} + [\text{NPO} \cdot \text{BF}_3] \overset{K_{DAL}}{\rightleftharpoons} [\text{anthracene} \cdot \text{NPO} \cdot \text{BF}_3] \quad (3)$$

Quantitative treatment of the dependence of this band intensity on the concentrations of donor, acceptor and Lewis acid was consistent with equilibrium in eqn (3), and it afforded the equilibrium constant: K_{DAL} = [anthracene·NPO·BF_3]/[anthracene] [NPO·BF_3] = 1.0 M^{-1} (Table 3).

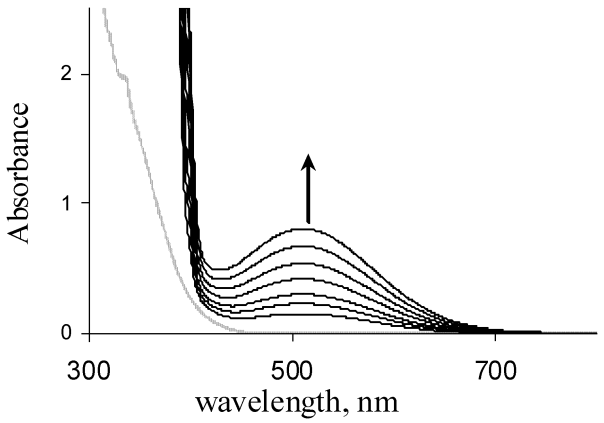

Fig. 8 Spectral changes accompanying addition of anthracene donor (from 0.0 to 0.14 M) to the dichloromethane solutions containing 0.015 M of NPO and 0.030 M of BF_3. [Note: dotted line represents a spectrum of NPO·BF_3 adduct.]

Addition of other aromatic donors to the dichloromethane solutions containing NPO and BF_3 resulted in appearance of similar absorption bands in the visible range indicating formation of the complexes analogous to those in eqn (3). Mulliken correlation between the absorption band energies (E_{CT}) of these complexes and the oxidation potentials of the donors in Fig. 9 (with correlation coefficient of 0.97) confirms the charge-transfer nature of the [D·NPO·BF_3] associates.[29]

Analogous charge-transfer absorption bands in the visible range were observed in electronic spectra of the solutions containing the same donors and [NQO·BF_3] adducts. In comparison, addition of the very strong TMPD donor to the solution containing mixture of either NPO or NQO and BF_3 resulted in appearance of the spectrum with peaks at 567 and 617 nm characteristic of corresponding $TMPD^{+\bullet}$ cation radicals.[6] Similar formation of cation radicals was observed upon addition of tetrathiafulvalene (TTF) or phenothiazine (PTZ) donors to the solutions containing mixtures of *N*-oxide (NPO or NQO) and BF_3 Lewis acid (*vide infra*).

Thus, UV-Vis spectral measurements indicated that complexation of *N*-oxide acceptor with Lewis acid results in increased stability of their complexes with organic donors and significant red shift of the charge-transfer absorption bands of their complexes (which allow measurements of these bands in the systems with relatively weak donors) and/or in oxidation of the strong donors. These data point out significant increase

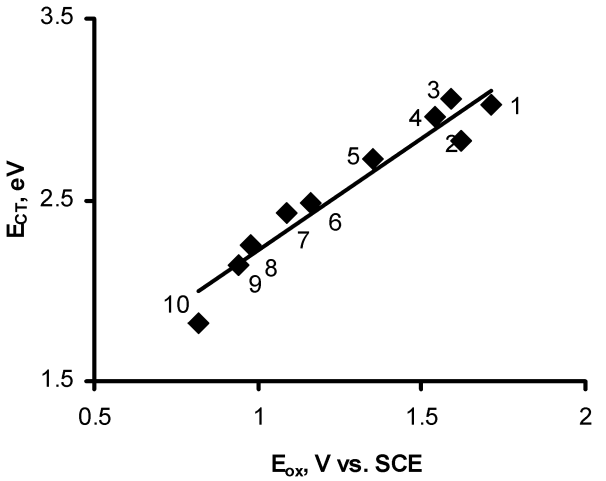

Fig. 9 Mulliken correlation between energies of absorption bands of [D·NPO·BF_3] complexes and oxidation potentials of donors. D = pentamethylbenzene (1), hexamethylbenzene (2), hexaethylbenzene (3), naphthalene (4), 1,4-dimethoxybenzene (5), pyrene (6), anthracene (7), 9,10-dimethoxyanthracene (8), 9,10-dimethylanthracene (9), and octamethylbiphenylene (10) (see Table S4 (ESI†) for details).

of acceptor strength of [NXO·BF_3] adducts, as compared to the isolated NXO *N*-oxide, which was further evaluated, as follows.

3.3 Electrochemical and spectral evaluations of the acceptor strength of [NXO·BF_3] adducts

Cyclic voltammetry studies (see Fig. S5 in ESI†) reveal that NQO and NPO *N*-oxides are characterized in dichloromethane by quasi-reversible reduction potentials of 0.81 and 0.87 V *vs.* SCE, respectively, which point to moderate acceptor strengths of these molecules. Similar measurements of the dichloromethane solution of boron trifluoride revealed irreversible reduction waves at about −0.5 V *vs.* SCE (Fig. S3, ESI†). In comparison, cyclic voltammograms of dichloromethane solutions containing mixtures of BF_3 and either NPO or NQO *N*-oxides show three irreversible reduction waves (Fig. S5, ESI†). In each case, the first of these waves appears at about −0.3 V *vs.* SCE, *i.e.* it is shifted in a positive direction as compared to the position of reduction waves of isolated BF_3, NPO or NQO acceptors. We tentatively assigned the waves at −0.3 V *vs.* SCE to the irreversible reduction of [NXO·BF_3] adducts.[30] However, the irreversible character of the electrochemical processes in the solutions containing NXO–BF_3 mixtures hindered quantitative analysis of effects of BF_3 coordination. As such, we turned to the spectral data for the evaluation of acceptor strength of [NXO·BF_3] adducts.

According to Mulliken and Person, absorption band energies of charge-transfer complexes of the same donor are directly related to the acceptor strengths.[29] Thus, the red shift of the charge-transfer band maxima of [anthracene·NPO·BF_3] associate (511 nm or 2.43 eV) relative to that of [anthracene·NPO] complexes (~425 nm or 2.92 eV) points out that the acceptor strength of the [NPO·BF_3] adduct is enhanced by ~0.5 V as compared to the NPO molecule. [Note that the intense 386 nm absorption band of NQO acceptor hinders measurements of its binary [donor, NQO] complexes and, thus, their spectral comparison with corresponding ternary complexes.]

Alternative estimations of acceptor strengths of the [NXO·BF_3] adducts were obtained using Mulliken correlations for complexes of pyrene and anthracene donors with various conventional organic acceptors. Indeed, charge-transfer associates between either of these donors and many organic acceptors are well known in the literature.[29,31] Absorption band energies of these complexes (which were reported earlier or measured in current work, see Table S5 in ESI†) demonstrate typical Mulliken correlations with reduction potentials of acceptors (Fig. 10). The placement of the energies of absorption bands of [pyrene·NPO·BF_3] and [pyrene·NQO·BF_3] complexes (2.43 and 2.32 eV, respectively) onto the Mulliken correlation for pyrene donor (as illustrated in Fig. 10A) afforded reduction potentials of [NPO·BF_3] and [NQO·BF_3] adducts of −0.38 V and −0.33 V, respectively. The same procedure with [anthracene·NPO·BF_3] and [anthracene·NQO·BF_3] associates in Fig. 10B led to similar numbers of −0.37 and −0.29 V for [NPO·BF_3] and [NQO·BF_3] adducts, respectively. These values are shifted by ~0.5 V in a positive direction as compared to the reduction potentials of the isolated NPO and NQO acceptors, which is in reasonable agreement with the electrochemical evaluations based on CV data for NPO–BF_3 and NQO–BF_3 mixtures.

3.4 Synergetic oxidation of organic donors in solution with NQO–BF_3 or NQO–BF_3 pairs

Spectral studies of dichloromethane solutions of strong TMPD, TTF or phenothiazine donors and either NQO or NPO *N*-oxides revealed absorption bands of corresponding charge-transfer complexes, and no indication of redox products (*vide supra*). Addition of BF_3 to these solutions led to their intense coloration and UV-Vis measurements showed appearance of the characteristic spectra of corresponding cation radicals. For example, Fig. 11 demonstrates that the visible range of the spectrum of 1 mM dichloromethane solution of phenothiazine donor and either 5 mM of NPO or 10 mM of BF_3 is essentially clear at $\lambda > 550$ nm (dash line). However, addition of a third component resulted in the fast appearance of the characteristic spectrum of phenathiazine cation radical (red line). At higher concentrations of PTZ, NPO and BF_3, their reactions resulted in precipitation of black $PTZ^{+\bullet}BF_4^-$ salt and GC-MS analysis indicated formation of 4,4′-diazopyridine *N*,*N*′-dioxide. Spectral titration (see Fig. S6 in ESI† for details) suggested that this reaction occurs according to eqn (4):

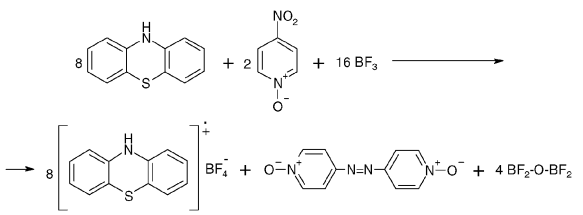

(4)

Similar results were obtained in the solutions containing NQO *N*-oxide, BF_3 and phenothiazine. These data indicate that simultaneous presence of BF_3 and NXO facilitates oxidation of

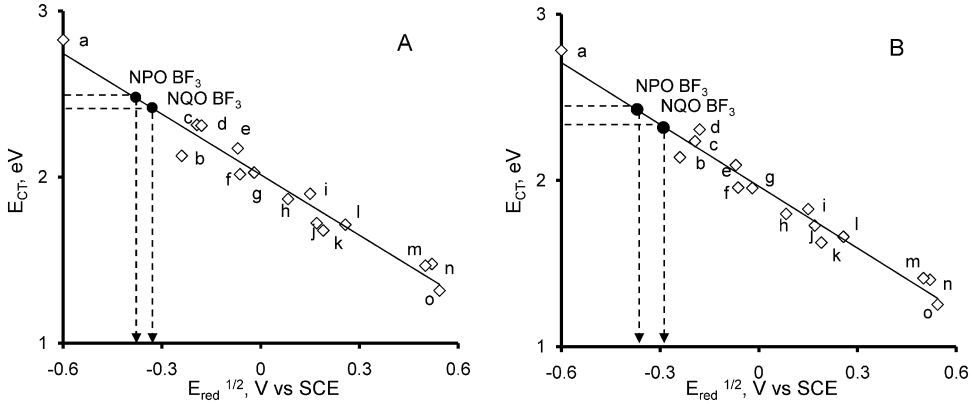

Fig. 10 Mulliken correlations for the complexes of various acceptors with pyrene (A) and anthracene (B): (a) 1,3,5-trinitrobenzene; (b) tetracyanopyrazine; (c) 2,6-dichloro-*p*-benzoquinone; (d) tropylium; (e) fluoranil; (f) *p*-bromanil; (g) *p*-chloranil; (h) *o*-bromanil; (i) *o*-chloranil; (j) tetracyanoethylene; (k) tetracyanoquinodimethane; (l) 2,3-dicyano-*p*-benzoquinone; (m) dibromodicyano-*p*-benzoquinone; (n) 2,3-dichloro-5,6-dicyano-*p*-benzoquinone; (o) tetrafluorotetracyanoquinodimethane (see Table S5 in ESI† for details).

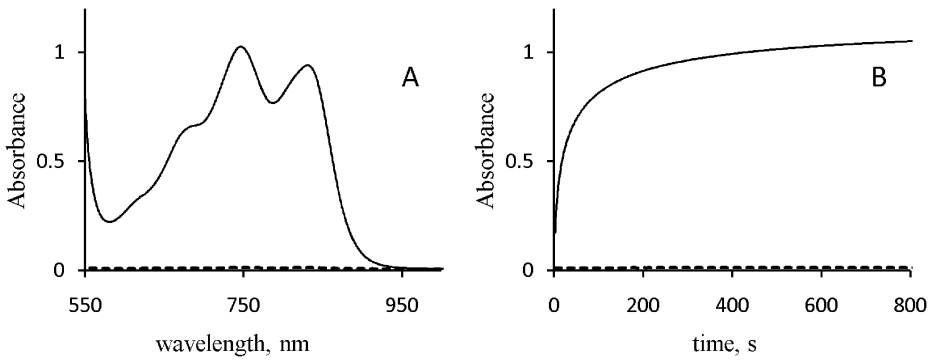

Fig. 11 (A) Spectra of dichloromethane solutions of 1 mM of PTZ with either 10 mM BF_3 or 5 mM of NPO (solid line) and 1 mM of PTZ, 5 mM of NPO and 10 mM of BF_3 (dash line) and (B) time dependence of 745 nm absorption of the solutions of 1 mM of PTZ in dichloromethane upon addition of: 10 mM of BF_3 (solid line), 10 mM of BF_3 and 5 mM of NPO (dash line).

phenothiazine to the corresponding $PTZ^{+\bullet}$ cation radical, and this process is accompanied by complex transformation of both Lewis acid *N*-oxides. [Note that rigorous study of redox process stoichiometries requires isolation of BF_2–O–BF_2, *etc*., and is beyond the scope of current work.] Similar appearance of cation radical spectra was observed in the ternary systems containing NPO, BF_3 and TTF or TMPD donors, as well as in the mixtures containing NQO, BF_3 and either phenothiazine or TTF or TMPD donor. As such, this chemical process (as well as analogous reaction with TTF and TMPD) can be described as synergetic oxidation of strong organic donors by NXO acceptor and Lewis acid.

Comparison of the oxidation potential of phenothiazine (0.59 V *vs*. SCE) with reduction potentials of [NXO·BF_3] adducts (about −0.3 V *vs*. SCE) indicates that PTZ + [NXO·BF_3] → $PTZ^{+\bullet}$ + $[NXO{\cdot}BF_3]^{-\bullet}$ electron transfer is strongly endergonic (ΔG_{ET} > 20 kcal M^{-1}). Thus, the free-energy gain necessary for the facile proceeding of phenothiazine oxidation is, in fact, provided by the follow-up reactions. Furthermore, the fast proceeding of the reaction ($\tau_{1/2} \approx 10$ s) indicates that the rate-limiting activation barrier for the whole process is lower than the energy associated with the intermediate formation of the separated $PTZ^{+\bullet}$–$[NPO{\cdot}BF_3]^{-\bullet}$ pair. These data suggest that follow-up reactions proceed directly from the successor complex for electron transfer as shown in Chart 2, (where D = PTZ, TMPD or TTF donors, and A = [[NXO·BF_3] adducts]). Stabilization of the successor complex by electrostatic interaction and/or electronic coupling within the ion-radical pair apparently decrease endergonicity of the electron-transfer step and thus attenuate the barrier $\Delta G^{\neq}$ for the overall process, as compared to the formation of the separate $D^+ + A^-$ pair.[6,32]

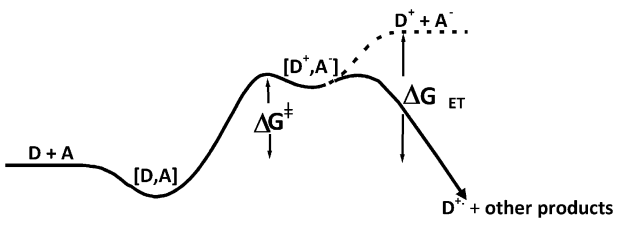

Chart 2

4. Conclusions

Spectral studies of the binary and ternary complexes involving *N*-oxides, BF_3 and organic donors, as well as their structural measurements (showing π-complexation of donor to the aromatic segment of the *N*-oxide moiety) and frontier orbital calculations (which revealed the LUMO of NXO·BF_3 adducts concentrating on *N*-oxide), indicate that optical and thermal electron transfer in these systems occurs from the donor to the *N*-oxide moiety. Acceptor strengths of the *N*-oxides are considerably enhanced by the Lewis acid coordination, and this enhancement is vital for the synergetic oxidation of organic donors. While the electron-transfer step in such ternary systems still remains quite endergonic even with strong organic donors, the overall redox process is apparently facilitated by free-energy gain from follow-up reactions, as well as by formation of donor–acceptor associates and ion-radical pairs.

Acknowledgements

We thank the R. A. Welch Foundation for financial support.

References

1 *Lewis acid in organic synthesis*, ed. H. Yamamoto, Wiley-VCH, Verlag, 2000.
2 *Selectivity in Lewis Acid Promoted Reactions*, ed. M. Sanelli and J.-M. Pons, CRC Press, Boca Raton, 1995.
3 A. Corma and H. Garcia, *Chem. Rev.*, 2002, **102**, 3837.
4 S. Fukuzumi, *Org. Biomol. Chem.*, 2003, **1**, 609; J. Yuasa, T. Suenobu and S. Fukuzumi, *ChemPhysChem*, 2006, **7**, 942; J. Yuasa, S. Yamada and S. Fukuzumi, *Chem.–Eur. J.*, 2008, **14**, 1866.
5 N. Sutin, *Prog. Inorg. Chem.*, 1983, **30**, 441.
6 S. V. Rosokha and J. K. Kochi, *Acc. Chem. Res.*, 2008, **41**, 641; S. V. Rosokha, D. Sun and J. K. Kochi, *J. Phys. Chem. B*, 2007, **111**, 6555; S. V. Rosokha and J. K. Kochi, *J. Am. Chem. Soc.*, 2007, **129**, 3683.
7 H. C. Brown and M. Grayson, *J. Am. Chem. Soc.*, 1953, **75**, 6285.
8 T. Okano, A. Takadate and T. Kano, *Jpn. J. Cancer Res.*, 1969, **60**, 557; A. V. Ryzhakov, *Russ. J. Gen. Chem.*, 1997, **67**, 808.
9 S. A. Winkle and I. Tinoko, *Biochemistry*, 1979, **18**, 3833.
10 S. Miyamoto, Y. Yasui, M. Kim, S. Sugie, A. Murakami, R. Ishigamori-Suzuki and T. Tanaka, *Carcinogenesis*, 2007, **29**, 418; M. Itjima, K. Mihara, T. Kondo, T. Tsuji, C. Ishioka and M. Namba, *Int. J. Cancer*, 1996, **66**, 698; R. Mirzayans, S. Bashir, D. Murray and M. C. Paterson, *Carcinogenesis*, 1999, **20**, 941.
11 H. B. Han, Q. Z. Pan, B. L. Zhang, J. Li, X. M. Deng, Z. X. Lian and N. Li, *Toxicology*, 2007, **230**, 151; C. E. Ogburn, J. Oshima, M. Poot, R. Chen, K. A. Gollahon, P. S. Rabinovitch and G. M. Martin, *Hum. Genet.*, 1997, **101**, 121; R. A. Schoop, R. J. Baatenburg de Jong and M. N. Noteborn, *Cancer Biol. Ther.*, 2008, **7**, 1368.
12 P. Srinisavan, S. Suchalatha, P. V. A. Babu, R. S. Devi, S. Narayan, K. E. Sabitha, D. Shymala and S. Chennam, *Chem.-Biol. Interact.*, 2008, **172**, 224; C. Matar, S. S. Nadathur, A. T. Bakalinsky and J. Goulet, *J. Dairy Res.*, 1997, **80**, 1965.
13 E. Ochiai, *Aromatic Amine Oxides*, Elsevier, Amsterdam, 1967.
14 A. V. Ryzhakov and L. L. Rodina, *Heterocycles*, 2008, **75**, 2367; A. V. Ryzhakov, V. P. Andreev and L. L. Rodina, *Heterocycles*, 2003, **60**, 419; V. P. Andreev and Y. P. Nizhnik, *Russ. J. Org. Chem.*, 2001, **37**, 141.
15 Y. P. Nizhnik, V. P. Andreev and B. Z. Belashev, *Russ. J. Org. Chem.*, 2008, **44**, 1824; V. P. Andreev and A. V. Ryzhakov, *Chem. Heterocycl. Compd.*, 1994, **30**, 938.
16 The term "ternary" hereinafter refers to a number of chemically distinct components in the complex, *i.e.* an amphoteric *N*-oxide (NXO), a π-donor (*e.g.* pyrene) and a Lewis acid (ν-acceptor: BF_3).
17 A. B. Burg and J. H. Bickerton, *J. Am. Chem. Soc.*, 1945, **67**, 2261.
18 E. Ochiai, *J. Org. Chem.*, 1953, **18**, 534.
19 D. D. Perrin, W. L. Armarego and D. R. Perrin, *Purification of Laboratory Chemicals*, Pergamon, New York, 1980.
20 H. A. Benesi and J. H. Hildebrand, *J. Am. Chem. Soc.*, 1949, **71**, 2703; R. S. Drago, *Physical Methods in Chemistry*, Saunders Co, Philadelphia, 1977.
21 S. V. Rosokha and J. K. Kochi, *J. Am. Chem. Soc.*, 2001, **123**, 8985.
22 M. J. Frisch, G. W. Trucks, H. B. Schlegel, G. E. Scuseria, M. A. Robb, J. R. Cheeseman, V. G. Zakrzewski, J. A. Montgomery, Jr., R. E. Stratmann, J. C. Burant, S. Dapprich, J. M. Millam, A. D. Daniels, K. N. Kudin, M. C. Strain, O. Farkas, J. Tomasi, V. Barone, M. Cossi, R. Cammi, B. Mennucci, C. Pomelli, C. Adamo, S. Clifford, J. Ochterski, G. A. Petersson, P. Y. Ayala, Q. Cui, K. Morokuma, P. Salvador, J. J. Dannenberg, D. K. Malick, A. D. Rabuck, K. Raghavachari, J. B. Foresman, J. Cioslowski, J. V. Ortiz, A. G. Baboul, B. B. Stefanov, G. Liu, A. Liashenko, P. Piskorz, I. Komaromi, R. Gomperts, R. L. Martin, D. J. Fox, T. Keith, M. A. Al-Laham, C. Y. Peng, A. Nanayakkara, M. Challacombe, P. M. W. Gill, B. G. Johnson, W. Chen, M. W. Wong, J. L. Andres, C. Gonzalez, M. Head-Gordon, E. S. Replogle and J. A. Pople, *GAUSSIAN 98 (Revision A.11)*, Gaussian, Inc., Pittsburgh, PA, 2001.
23 G. M. Sheldrick, *SADABS (Ver. 03)*, 2000; G. M. Sheldrick, *SHELXS 97*, University of Göttingen, Germany, 1997.
24 H. Feinberg, I. Columbus, S. Cohen, M. Rabnovitz, H. Selig and G. Shoham, *Polyhedron*, 1993, **12**, 2913; S.-Z. Zhang, S. Sato, E. Horn and N. Furukava, *Heterocycles*, 1998, **48**, 227.
25 With sp^2-hybridized oxygen, this dihedral angle is expected to be close to zero (Fig. S7 in ESI†). Note that use of the N–O–B angle as an indicator of the oxygen hybridization is hindered by its sensitivity to steric factors (Table S6 in ESI†).
26 The NPO molecule can be presented as a hybrid of two major resonance contributors, *i.e.* (A) benzenoid structure with nearly equivalent bond lengths in the aromatic ring, as well as single N–O and C–NO_2 bonds and (B) quinonoid structures with two double/four single bonds in the ring, as well as double N–O and C–NO_2 bonds (Fig. S8 in ESI†). The higher contribution of the quinonoid structure results in larger bond length variation in the ring, longer N–O and C–NO_2 bonds and larger nitro group twist angle (and *vice versa*). Quantitatively, it can be evaluated as: $q = 1/n\ \Sigma\{\Delta d_i(\mathrm{NPO})/\Delta d_i(\mathrm{Q})\}$, where Δd^i refers to the difference of a particular bond in the NPO molecule and in the hypothetical benzenoid structure, $\Delta d^i(\mathrm{Q})$—the difference of the same bond in the benzenoid and quinonoid structures, and n is a number of bonds (so $q = 0$ and $q = 1$ correspond to benzenoid structure A and to quinonoid structure B, respectively). Compare: J. M. Lu, I. S. Neretin, S. V. Rosokha and J. K. Kochi, *J. Am. Chem. Soc.*, 2006, **128**, 16708.
27 P. Coppens and M. S. Lehmann, *Acta Crystallogr., Sect. B: Struct. Crystallogr. Cryst. Chem.*, 1976, **32**, 1777.
28 Y. P. Nizhnik, S. V. Rosokha, J. J. Lu and J. K. Kochi, *CrystEngComm*, 2009, DOI: 10.1039/b905845a.
29 R. S. Mulliken and W. B. Person, *Molecular Complexes*, Wiley, New York, 1969; *Molecular Association*, ed. R. Foster, Academic Press, New York, 1975, vol. 1.
30 The increase of concentration of BF_3 resulted in an intensity increase of the wave at −0.3 V and a decrease of the intensity of the −0.8 V wave in the cyclic voltammograms of the NXO–BF_3 solutions, which accords with the increase of the fraction of BF_3-coordinated *N*-oxide. However, the irreversible character of the redox processes hindered rigorous analysis and assignment of these data.
31 V. Ganesan, S. V. Rosokha and J. K. Kochi, *J. Am. Chem. Soc.*, 2003, **125**, 2559.
32 S. V. Rosokha and J. K. Kochi, *J. Org. Chem.*, 2002, **67**, 1727; S. V. Rosokha, S. M. Dibrov, T. Y. Rosokha and J. K. Kochi, *Photochem. Photobiol. Sci.*, 2006, **5**, 914.